

# Disordered contact process with asymmetric spreading

Róbert Juhász

*Institute for Solid State Physics and Optics, Wigner Research Centre for Physics, H-1525 Budapest, P.O. Box 49, Hungary\**

(Dated: October 5, 2012)

An asymmetric variant of the contact process where the activity spreads with different and independent random rates to the left and to the right is introduced. A real space renormalization scheme is formulated for model by means of which it is shown that the local asymmetry of spreading is irrelevant on large scales if the model is globally (statistically) symmetric. Otherwise, in the presence of a global bias in either direction, the renormalization method predicts two distinct phase transitions, which are related to the spreading of activity in and against the direction of the bias. The latter is found to be described by an infinite randomness fixed point while the former is not.

PACS numbers: 05.70.Ln, 64.60.Ak, 02.50.Ey

*This paper is dedicated to Ferenc Iglói on the occasion of his 60th birthday.*

## I. INTRODUCTION

The contact process [1, 2] is a simple model of an epidemic that is defined on a lattice of binary variables which can be either inactive (healthy) or active (infected). The dynamics consist of two kinds of competing moves: infection of adjacent healthy sites by infected ones and spontaneous healing of the latter. Besides being a starting point for designing more realistic models of epidemics it is a thoroughly studied (but non-soluble), paradigmatic model of systems undergoing a non-equilibrium phase transition from a fluctuating phase to an absorbing one [3–5]. In the case of translational invariance, the phase transition belongs to the universality class of directed percolation [4], although this type of critical behavior is rarely observed in real systems [6] since, according to the Harris criterion, it is unstable against weak quenched disorder in dimensions  $d < 4$  [7]. The understanding of the behavior of the model in the presence of quenched disorder is therefore of great importance. Early Monte Carlo simulations showed, in agreement with phenomenological considerations, that the disorder leads to anomalous dynamics outside of the critical point [7–9] and, at the critical point, the different observables scale with some power of the logarithm of time rather than the time itself [8]. Below the critical point, namely, the density of active sites and the survival probability show a power-law decay with dynamical exponents varying continuously with the control parameter, while, above the critical point, the size of the set of active sites is growing sub-linearly in one dimension when the process was started from a single active seed [10]. These phases are analogues of the disordered and ordered Griffiths phases of magnetic systems [11], respectively, and the slow dynamics are related to the occurrence of so

called rare regions which are locally in the opposite phase with respect to the majority of the system. In the sub-critical Griffiths phase, the rare regions are locally super-critical clusters and, although, being exponentially rare (in their size), due to their exponentially large extinction time they are able to change the usual exponential temporal decay of the density to an algebraic one. Instead, in the super-critical Griffiths phase, the creeping motion of the front of the active cluster is caused by rare sub-critical regions which impede the spreading of activity for long times. A substantial progress in the quantitative description of the critical point was the adaptation of a strong disorder renormalization group (SDRG) scheme [12] to the model by Hooyberghs, Iglói and Vanderzande [13]. The formal description of the model by the SDRG is essentially identical with that of the random transverse-field Ising model [14] and, in one dimension, yields logarithmic critical dynamics and the complete set of critical exponents which are universal, i.e. independent of the form of disorder. These predictions were confirmed by Monte Carlo simulations and found to be valid also for relatively weak disorder, where the initial steps of the SDRG procedure are highly approximative [15].

In the SDRG treatment of the model, the activity is assumed to spread through a given link in both directions with the same rate (that varies from link to link), while in the numerical simulations, slightly differently, the infection from a given site occurs in both directions with equal rates. So, in the latter case, the spreading of activity through a link is non-symmetric (or biased) and one may ask whether this case can be treated by an appropriately generalized SDRG scheme. More generally, one could pose the same question as well as the question what is the nature of the phase transition in an asymmetric variant of the disordered contact process where the infection rates  $\lambda_{ij}$  assigned to a directed link  $(i, j)$  are completely uncorrelated random variables. In case of a translationally invariant model with a bias (i.e. different infection rates in the two directions) the phase transition is known to belong to the directed percolation universality class as in the unbiased model [16]. But, the breaking of the translation symmetry, for instance, by putting an active wall to the system, leads to differences

---

\*Electronic address: juhasz.robert@wigner.mta.hu

compared to the unbiased case, see Ref. [17]. So, one expects that in the simultaneous presence of a global bias and quenched disorder the nature of phase transition is different from that of the homogeneous, biased contact process.

The aim of the present work is to study the disordered, asymmetric contact process in one dimension by working out and applying an SDRG scheme. We will show that, if the model is statistically symmetric, then the local asymmetry of links is irrelevant and the critical behavior is identical to that of the symmetric model. If, however, the model is globally asymmetric, i.e. there is a bias in either direction, two distinct phase transitions arise, which are related to the spreading of activity in and against the direction of the bias. These results will be expounded in the rest of the paper, which is organized as follows. In Section II, the precise definition of the model is given and the SDRG scheme is introduced. The case of weak asymmetry is analyzed in Section III, while the behavior of the globally symmetric and the biased model is discussed in Section IV and Section V, respectively. The results are summarized in Section VI and some calculations are presented in the Appendix.

## II. THE ASYMMETRIC CONTACT PROCESS AND THE SDRG SCHEME

Let us consider a one-dimensional lattice where each site can be in two states: either active (infected) or inactive (healthy). The asymmetric contact process is a continuous-time Markov process on this state space, which consists of the following transitions occurring independently. Active sites become inactive with a rate  $\mu_i$  on site  $i$ , and, if site  $i$  is active, it infects the neighboring site on its right with a rate  $\lambda_i$  and the neighboring site on its left with a rate  $\kappa_{i-1}$ . The rates  $\lambda_i$  and  $\kappa_i$  will be termed as forward and backward infection rates, respectively. The transition rates  $\{\mu_i, \lambda_i, \kappa_i\}$  are time-independent random variables, the distribution of which will be specified later.

The SDRG transformation of the disordered, symmetric contact process[13] is a real space renormalization transformation which sequentially eliminates the quickly relaxing degrees of freedom and replaces the original system by a reduced one that, however, preserves the slowly relaxing degrees of freedom of the original system. Formally, finite blocks of sites are considered, the time evolution of which are governed by a master equation

$$\partial_t \mathbf{P} = \mathbf{P}Q, \quad (1)$$

where the probabilities of states are arranged in the row vector  $\mathbf{P}(t) = (p_1(t), p_2(t), \dots)$  and  $Q$  is the rate matrix (or infinitesimal generator) of the process. In the SDRG procedure, the blocks are selected in which the spectrum of  $Q$  shows a separation of niveous. Then the higher-lying states are discarded and the block is replaced by a simpler one having the same low-lying niveous. For

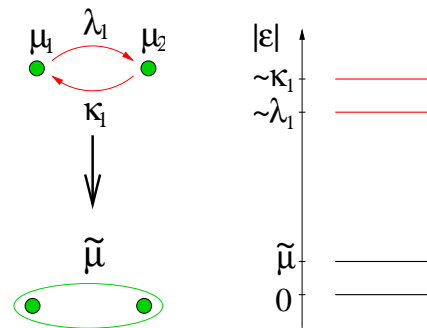


FIG. 1: Left: Illustration of the merging of two sites connected by a link with large infection rates. Right: Schematic spectrum of the rate matrix of the two-site block.

the symmetric model, there are two types of reduction steps, and this structure of the SDRG with appropriate modifications will be kept also for the asymmetric contact process.

### A. Cluster merging

First, let us consider an isolated block of two sites shown in Fig. 1, and assume that the infection rates in both directions are much larger than the recovery rates,  $\lambda_1, \kappa_1 \gg \mu_1, \mu_2$ . In this case the two sites are most of the time either both active or both inactive. This suggests that the block can be substituted by a single giant site (or cluster) with an appropriate recovery rate  $\tilde{\mu}$ . Indeed, analyzing the spectrum of the rate matrix of the block, see the Appendix, one obtains that the two higher-lying niveous are well separated from the two lower-lying ones. Note that at least one of the eigenvalues is always zero since the rate matrix is a stochastic matrix. For an isolated single site with recovery rate  $\tilde{\mu}$ , the only non-trivial eigenvalue is  $-\tilde{\mu}$ . So, the effective recovery rate of the giant site is identified with the magnitude of lowest non-trivial eigenvalue of the rate matrix or, equivalently the (in magnitude) smallest root of Eq. A2. If  $\lambda_1, \kappa_1 \gg \mu_1, \mu_2$ , one obtains the approximate form:

$$\tilde{\mu} \simeq \frac{\mu_1 \mu_2}{\omega_1}, \quad (2)$$

where the combined infection rate  $\omega_i$  is defined as

$$\omega_i \equiv \frac{\lambda_i \kappa_i}{\lambda_i + \kappa_i}. \quad (3)$$

Note that if the infection rates  $\lambda_i$  and  $\kappa_i$  differ by orders of magnitudes then  $\omega_i$  gives roughly the smaller one of them. We can see that this type of reduction of the two-site block to a single site is justified only if *both* infection rates on the link (or, equivalently  $\omega_i$ ) are much larger than the recovery rates [29], and the life-time of activity in the two-site block is controlled by the smallest infection rate. Consequently, in a totally asymmetric

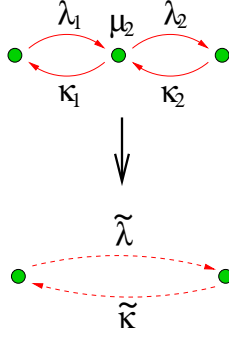


FIG. 2: Illustration of the elimination of a site with a large recovery rate  $\mu_2$ .

contact process where infection spreads unidirectionally, giant clusters with low decay rate never form, hence no rare region effects are expected to emerge (unless the initial recovery rates are not bounded away from zero).

Besides the transition rates, we also keep track of the mass of clusters, i.e. the number  $n$  of original sites comprised by a giant site. Obviously, this quantity transforms as

$$\tilde{n} = n_1 + n_2. \quad (4)$$

### B. Cluster elimination

Next, let us consider an isolated three-site block shown in Fig. 2, where the recovery rates on the two lateral sites are zero. If the recovery rate  $\mu_2$  is much larger than the infection rates,

$$\mu_2 \gg \lambda_1, \kappa_1, \lambda_2, \kappa_2, \quad (5)$$

the middle site will be most of the time inactive and transmits infection only during its rare flashes of activity. It is thus reasonable to eliminate this site and connect the lateral sites by a direct link with some effective (reduced) infection rates. Solving the eigenvalue problem of the rate matrix of the block, see the Appendix and Fig. 3, one sees that the higher-lying 4 niveous, being in the order of  $\mu_2$ , are well separated from the lower-lying 4 niveous among which two niveous have zero eigenvalue. This lower-lying bunch of niveous is to be compared with the spectrum of a two-site block with infection rates  $\tilde{\lambda}, \tilde{\kappa}$  and zero recovery rates. The eigenvalues of the latter are  $(0, 0, -\tilde{\lambda}, -\tilde{\kappa})$ , so the effective infection rates of the three-site block are identified as the magnitude of the two lowest-lying non-trivial eigenvalues. If the condition in Eq. (5) is fulfilled, we have

$$\tilde{\lambda} = s_\lambda \left( 1 - \sqrt{1 - \frac{\lambda_1 \lambda_2}{s_\lambda^2}} \right), \quad s_\lambda \equiv \frac{\mu_2 + \lambda_1 + \lambda_2}{2} \quad (6)$$

$$\tilde{\kappa} = s_\kappa \left( 1 - \sqrt{1 - \frac{\kappa_1 \kappa_2}{s_\kappa^2}} \right), \quad s_\kappa \equiv \frac{\mu_2 + \kappa_1 + \kappa_2}{2} \quad (7)$$

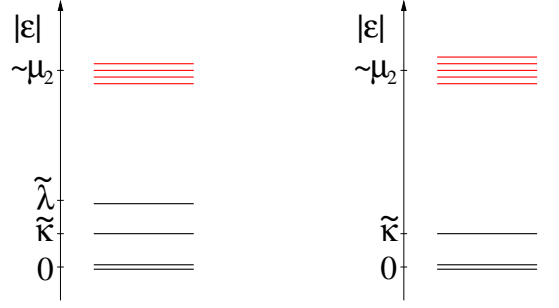


FIG. 3: Schematic spectrum of the rate matrix of a three-site block in the case of complete separation (left) and partial separation (right).

and obtain the approximate expressions

$$\tilde{\lambda} \simeq \frac{\lambda_1 \lambda_2}{\mu_2}, \quad \tilde{\kappa} \simeq \frac{\kappa_1 \kappa_2}{\mu_2}, \quad (8)$$

while the other non-trivial eigenvalues are  $O(\mu_2)$ . Here, we speak of a *complete separation* of niveous. As we will see later, the cluster elimination step will be applied in the SDRG procedure only if  $\mu_2 > \omega_1, \omega_2$  and, due to the broad distribution of rates we have typically  $\omega_i \approx \min\{\lambda_i, \kappa_i\}$ . If the two links of the block are biased in opposite directions, e.g.  $\lambda_1, \kappa_2 \ll \mu_2$  and  $\kappa_1, \lambda_2 > \mu_2$ , then the spectrum still displays a weaker form of complete separation [30]. But if the two links are biased in the same direction, e.g. to the right,

$$\lambda_1, \lambda_2 > \mu_2, \quad \kappa_1, \kappa_2 \ll \mu_2, \quad (9)$$

then only the lowest (non-trivial) eigenvalue separates from the higher ones. The corresponding rate  $\tilde{\kappa} \simeq \kappa_1 \kappa_2 / \mu_2$  can still be interpreted as an effective spreading rate of the activity from right to left but by this reduction, the information on how the activity spreads from left to right is lost. We call this situation a *partial separation* of levels.

We will also keep track of evolution of the number  $l$  of original links which are incorporated into the effective links. This quantity is dual to the mass of giant sites and transforms in the cluster elimination step as

$$\tilde{l} = l_1 + l_2. \quad (10)$$

### C. The SDRG scheme

After introducing the elementary reduction steps, we are in a position to formulate a SDRG scheme for the asymmetric contact process. First, the largest one among the rates  $\{\omega_i, \mu_i\}$ , which will be denoted by  $\Omega$ , is selected. If  $\Omega$  is a combined infection rate (recovery rate) then the cluster merging step (cluster elimination step) is performed. The above steps are then iteratively applied to the renormalized system. This recursive procedure gradually reduces the cut-off rate  $\Omega$ , which amounts to that,

roughly speaking, the fast processes occurring on a time scale shorter than  $\Omega^{-1}$  are eliminated. The basic dynamical relation between the time and the length scale can be inferred from the asymptotic dependence of the cut-off  $\Omega$  on the fraction of active (non-decimated) degrees of freedom [12]. Note that, if the model is symmetric ( $\lambda_i = \kappa_i$ ) the above SDRG procedure reduces to the that applied in Ref. [13].

Before we proceed with the analysis of the SDRG transformation, we need to recapitulate some of the results of the symmetric contact process obtained by the SDRG technique. For further details we refer the reader to Ref. [13]. In the case of the symmetric model, the distribution of the logarithm of rates is broadening without limits under the SDRG transformation, therefore the conditions of the approximative reduction steps are fulfilled better and better and the procedure becomes asymptotically exact. Due to that the rates at different sites remain independent provided they were so initially, it is sufficient to deal with the evolution of the probability of rates under the renormalization and the problem is analytically tractable. The asymptotic transformation of rates in Eqs. (2) and (8) is identical to that of the couplings and external fields of the random transverse-field Ising chain up to a constant factor which is irrelevant at the critical point [13]. The asymptotic solution of the renormalization equations of the latter problem at the critical point, which is at the self-dual point of the transformation, have been found in Ref. [14]. Here, in the so called *infinite randomness fixed-point* of the transformation, both the logarithm of infection and recovery rates scale as

$$|\ln \tilde{\lambda}| \sim |\ln \tilde{\mu}| \sim \xi^{1/2} \quad (11)$$

and the mass of clusters as well as the length of effective links grow as

$$\tilde{n} \sim \tilde{l} \sim \xi^{d_f}, \quad (12)$$

where  $d_f = (1 + \sqrt{5})/4 = 0.809 \dots$  is the fractal dimension of clusters. The Griffiths phase which is located on the sub-critical side of the critical point is characterized by a line of fixed points where the rates scale as

$$|\ln \tilde{\lambda}| \sim \xi, \quad \tilde{\mu} \sim \xi^{-z}, \quad (13)$$

while the mass and the length behave as

$$\tilde{n} \sim \ln \xi, \quad \tilde{l} \sim \xi. \quad (14)$$

The dynamical exponent  $z$  appearing here depends on the distribution of rates of the original model [19]. In the super-critical Griffiths phase  $\lambda$  and  $\mu$ , as well as  $n$  and  $l$  are interchanged in the above relations.

### III. WEAK ASYMMETRY

Returning to the asymmetric contact process, we introduce a control parameter which measures the magnitude

of infection rates relative to that of recovery rates by

$$\Delta \equiv \overline{\ln \omega_i} - \overline{\ln \mu_i}, \quad (15)$$

where the over-bar denotes an average over sites, and a local asymmetry parameter as

$$a_i \equiv \ln \lambda_i - \ln \kappa_i. \quad (16)$$

First, let us consider a weak, asymmetric perturbation of the symmetric model: the parameters  $a_i$  are uncorrelated random variables written in the form

$$a_i \equiv I \alpha_i, \quad (17)$$

where  $I$  is an infinitesimally small global constant and  $\alpha_i$  is  $O(1)$ . Let us assume, furthermore, that the transformation is close to the fixed-point, so that the approximate but asymptotically exact rules in Eqs. (2) and (8) can be used. Now, it is expedient to use the variables  $(\omega_i, a_i)$  instead of  $(\lambda_i, \kappa_i)$  in terms of which the old variables are expressed as  $\lambda_i = \omega_i(1 + e^{a_i})$  and  $\kappa_i = \omega_i(1 + e^{-a_i})$ . In a cluster elimination step these variables transform (asymptotically) as

$$\tilde{a} \simeq a_1 + a_2 \quad (18)$$

$$\tilde{\omega} \simeq f(a_1, a_2) \frac{\omega_1 \omega_2}{\mu_2}, \quad (19)$$

$$f(a_1, a_2) \equiv 1 + \frac{e^{a_1} + e^{a_2}}{1 + e^{a_1 + a_2}}, \quad (20)$$

while in a cluster merging step they still follow the rule given in Eq. (2). Since the parameters  $a_i$  are infinitesimal, we have  $f(a_1, a_2) = 2$  and the pair of variables  $\omega_i$  and  $\mu_i$  transforms autonomously (i.e. not influenced by the variables  $a_i$ ), identically to the infection rate and recovery rate of a symmetric contact process. As can be seen above, the asymmetry parameter  $a_i$  transforms in the same way as the length  $l_i$  of effective links given in Eq. (10). The only difference is in that the original parameters  $a_i$  have not necessarily the same sign, while we have  $l_i = 1$ . The renormalized asymmetry parameter  $\tilde{a}_i$  can thus be written as a sum of original variables  $a_i$  with  $\tilde{l}_i$  terms which are selected by the procedure independently of the parameters  $a_i$ .

The above renormalization scheme allows for two different scenarios of the evolution of the asymmetry parameters depending on the initial distribution of rates. There may be initial distributions biased to the left or to the right for which the asymmetry parameter  $\alpha_i$  averaged over sites tends to plus or minus infinity, respectively. Or it may tend to zero as the fixed-point of the transformation is approached. In the latter case, the system is statistically symmetric, although it is locally asymmetric. A sufficient condition for this is that the distribution of original infection rates is invariant under the interchange of  $\lambda$  and  $\kappa$ , i.e.

$$P(\lambda, \kappa) \equiv P(\kappa, \lambda). \quad (21)$$



This property will then be preserved by the renormalization. It is, however, not a necessary condition for the system being statistically symmetric but owing to the approximative nature of the renormalization far from the asymptotical region and that even the homogeneous model is non-integrable it is not possible to find a general condition in terms of the distribution of the initial rates.

On the basis of the above considerations, if the initial distribution of infection rates is biased so that the mean asymmetry is growing in magnitude, it must scale close to the fixed-point as the length:

$$\overline{\tilde{\alpha}(\xi)} \sim \overline{\tilde{l}(\xi)}. \quad (22)$$

But if the system is initially statistically symmetric, i.e.  $\overline{\tilde{\alpha}(\xi)} \rightarrow 0$  as the fixed-point is approached, then, according to the central limit theorem, the square of the variance of  $\tilde{\alpha}$  scales as the length:

$$\overline{\tilde{\alpha}^2(\xi)} \sim \overline{\tilde{l}(\xi)}. \quad (\overline{\tilde{\alpha}} \rightarrow 0) \quad (23)$$

Using now the results of the symmetric model quoted in the previous section, we obtain for the scaling of typical asymmetry parameter at the critical point  $\Delta = \Delta_0$

$$|\tilde{\alpha}(\xi)| \sim \xi^{d_f/2}, \quad \text{if } \overline{\tilde{\alpha}} \rightarrow 0 \quad (24)$$

$$\tilde{\alpha}(\xi) \sim \xi^{d_f}, \quad \text{otherwise.} \quad (25)$$

In the sub-critical Griffiths ( $\Delta < \Delta_0$ ) phase, we obtain

$$|\tilde{\alpha}(\xi)| \sim \xi^{1/2}, \quad \text{if } \overline{\tilde{\alpha}} \rightarrow 0 \quad (26)$$

$$\tilde{\alpha}(\xi) \sim \xi, \quad \text{otherwise,} \quad (27)$$

while in the super-critical Griffiths phase ( $\Delta > \Delta_0$ )

$$|\tilde{\alpha}(\xi)| \sim (\ln \xi)^{1/2}, \quad \text{if } \overline{\tilde{\alpha}} \rightarrow 0 \quad (28)$$

$$\tilde{\alpha}(\xi) \sim \ln \xi, \quad \text{otherwise.} \quad (29)$$

#### IV. THE STATISTICALLY SYMMETRIC MODEL

Next, we consider finite local asymmetry parameters but require that the distribution of  $a_i$  is not too broad so that its moments are finite. As we have seen above, the asymmetry parameter scales differently depending on whether the system is statistically symmetric or not. Let us consider first, the former case, which is guaranteed if Eq. (21) holds.

Assume temporarily that the initial asymmetry is finite but weak ( $I \ll 1$ ) so that, at least within a finite length scale  $\xi_0(I)$ , the system can be regarded as approximately symmetric. As the model is renormalized, the initially uncorrelated rates  $\lambda_i$  and  $\kappa_i$  become correlated since they are transformed simultaneously and on longer effective links both  $\tilde{\lambda}$  and  $\tilde{\kappa}$  are typically smaller than on shorter ones. If the system is critical, the typical asymmetry parameter starts to grow as  $|\tilde{a}| \equiv |\ln \tilde{\lambda} - \ln \tilde{\kappa}| \sim I \xi^{d_f/2}$ .

But the typical value and the width of the distribution of logarithmic rates themselves are increasing faster, see Eq. (11), since  $d_f/2 < 1/2$ . Consequently, if a combined infection rate  $\omega_i$  is much smaller than  $\mu_2$  in a cluster elimination step, then typically both  $\lambda_i$  and  $\kappa_i$  are much smaller than  $\mu_2$ . In other words, a complete separation of niveous is realized. Furthermore, taking the logarithm of Eq. (19), we can see that the term  $\ln f(a_1, a_2)$ , which is at most  $O(\xi^{d_f/2})$ , is negligibly small compared to the other terms on the r.h.s., which are  $O(\xi^{1/2})$ . Therefore the SDRG transformation can be continued beyond the scale  $\xi_0(I)$  and as the fixed-point is approached ( $\xi \rightarrow \infty$ ), the relative asymmetry parameter tends to zero with probability one,

$$\frac{\ln(\tilde{\lambda}_i/\tilde{\kappa}_i)}{\ln \tilde{\lambda}_i} \sim \xi^{(d_f-1)/2} \rightarrow 0, \quad (\Delta = \Delta_0) \quad (30)$$

and the system transforms asymptotically like the symmetric one. But this is not restricted to the critical point. Following the above reasoning and using Eq. (26), we obtain a vanishing relative asymmetry parameter in the sub-critical Griffiths phase,

$$\frac{\ln(\tilde{\lambda}_i/\tilde{\kappa}_i)}{\ln \tilde{\lambda}_i} \sim \xi^{-1/2} \rightarrow 0, \quad (\Delta < \Delta_0) \quad (31)$$

as well as, using Eq. (28), in the super-critical Griffiths phase:

$$\frac{\ln(\tilde{\lambda}_i/\tilde{\kappa}_i)}{\ln \tilde{\lambda}_i} \sim (\ln \xi)^{-1/2} \rightarrow 0. \quad (\Delta > \Delta_0) \quad (32)$$

So, we conclude that, in the statistically symmetric model, the local asymmetry becomes irrelevant in the fixed-point of the SDRG transformation, and, consequently, the large scale properties are identical to that of the symmetric model.

It is, however, difficult to answer whether for any type of initial distributions of transition rates the large scale properties of the system are described by the fixed-point of the SDRG transformation. For contributions to the unresolved question whether any weak initial disorder results in logarithmic critical scaling described by the infinite randomness fixed-point in the symmetric model we refer the reader to Refs. [13, 15, 20, 21]. In the asymmetric contact process this problem is made more difficult by introducing the extra parameter  $a_i$ . The numerical investigation of the SDRG scheme shows that not only weak but even relatively strongly asymmetric initial disorder, such as independent uniform distributions of the rates  $\lambda_i$ ,  $\kappa_i$  and  $\mu_i$ , drives the system to the infinite randomness fixed-point.

##### A. The site-symmetric model

We make a digression here on a special model studied by Monte Carlo simulations [15], where the infection spreads from each site in both directions with equal

rates, i.e.  $\lambda_i = \kappa_{i-1}$  for all  $i$ . As opposed to the earlier assumption, the initial asymmetry parameters are now correlated variables and it is easy to see that the sum of  $a_i$  over subsequent sites is independent from the number of terms:

$$\sum_{i=1}^n a_i = \ln(\lambda_1/\kappa_n). \quad (33)$$

Thus, one expects here a slower increase of the asymmetry parameter under renormalization than for the uncorrelated disorder. Assume for the sake of simplicity that the initial disorder is strong enough so that the asymptotic forms of the renormalization rules can be used. The renormalized asymmetry parameter of an arbitrary effective link is the sum of initial variables  $a_i$  of links which have been incorporated into the effective link via cluster eliminations. These links, when regarded in the original system, form a disconnected set due to the eventual cluster merging steps occurring during the renormalization. Each connected part of length  $n$  of this set gives a contribution given in Eq. (33) independently of  $n$  to  $\tilde{a}$ . So, the number of independent terms in  $\tilde{a}$  is given just by the number of connected components of the set of links rather than the total number of links. It is easy to obtain that the number of connected components  $c_i$ , which is initially 1 on each link, transforms in a cluster elimination step in the way:

$$\tilde{c} = \begin{cases} c_1 + c_2 - 1, & \text{if } n_2 = 1 \\ c_1 + c_2, & \text{if } n_2 > 1 \end{cases} \quad (34)$$

This is not much different from the transformation of the variable  $l_i$  given in Eq. (10) and, taking into account that the mass of clusters is increasing, the probability of finding a cluster with  $n = 1$  goes to zero as  $\xi \rightarrow \infty$ . So, the transformation rules of  $n$  and  $c$  are asymptotically identical and, consequently, the scaling of the asymmetry parameter follows the same laws as in the uncorrelated case given in Eqs. (30-32), and at most the prefactors are reduced.

## V. THE BIASED MODEL

In the remaining part of the paper we will discuss the case when the spreading of activity is biased to either direction, for example, if  $a_i > 0$  for all  $i$ , and will be interested in the possible fixed-points of the SDRG transformation. We have seen for infinitesimal asymmetry that  $\bar{\alpha} \rightarrow \infty$  in the biased model. For finite asymmetry, we will therefore have typically  $\tilde{\lambda}_i \gg \tilde{\kappa}_i$  on large scales and, consequently,  $\tilde{\omega}_i \simeq \tilde{\kappa}_i$  and  $f(\tilde{a}_1, \tilde{a}_2) \simeq 1$ .

### A. Griffiths phase

Assume now that the control parameter  $\Delta$  is small enough, such that the system is sub-critical and even

the forward rate  $\tilde{\lambda}$  is typically small compared to  $\tilde{\mu}$ , i.e.  $\tilde{\lambda}/\tilde{\mu} \rightarrow 0$ . In this case, we have a complete separation of niveous in cluster elimination steps and the variables  $\omega$  and  $\mu$  transform autonomously as

$$\tilde{\omega} \simeq \frac{\omega_1 \omega_2}{\mu_2}, \quad \tilde{\mu} \simeq \frac{\mu_1 \mu_2}{\omega_2}, \quad (35)$$

in cluster elimination and merging steps, respectively, whereas the asymmetry parameter in the former as  $\tilde{a} \simeq a_1 + a_2$ . The renormalized parameters under these transformations will scale asymptotically as

$$\begin{aligned} \ln \tilde{\omega}^{-1} &\simeq \ln \tilde{\kappa}^{-1} \sim \xi, \\ \tilde{\mu} &\sim \xi^{-z}, \\ \tilde{a} &\sim \xi, \end{aligned} \quad (36)$$

and flow to a line of fixed points parameterized by a non-universal dynamical exponent  $z$  that depends on the distribution of initial rates [19]. This line can be interpreted as the subcritical Griffiths phase, where the dynamics are described by power laws with distribution-dependent exponents.

As in the Griffiths phase of the symmetric model, a finite length scale  $\xi_1$  above which the renormalized recovery rates are typically larger than the renormalized combined infection rates can be defined. This length scale can be interpreted as the characteristic size of locally supercritical clusters. Beyond this scale,  $\xi \gg \xi_1$ , practically no cluster merging step occurs in the SDRG procedure. In the biased model at this length scale  $\xi \sim \xi_1$ , the backward rates  $\tilde{\kappa}$  are comparable with  $\tilde{\mu}$  but the forward rates  $\tilde{\lambda}$  are still larger than  $\tilde{\mu}$ . Similar to  $\xi_1$ , one can define a second length scale  $\xi_2 (> \xi_1)$  above which the recovery rates typically exceed even the forward rates. An interpretation of  $\xi_2$  can be given if the process starts from a single active site. In this case, the activity spreads to the right typically up to a finite distance  $\xi_2$ , where it is trapped until becoming extinct. Thus, the observables usually measured in simulations, such as the survival probability, are expected to have the same time dependence beyond a time scale corresponding to  $\xi_2$  as in the sub-critical Griffiths phase of the symmetric model.

### B. The lower phase transition and the weak-survival phase

When the control parameter  $\Delta$  is increased, both  $\xi_1$  and  $\xi_2$  increase and there must be a point  $\Delta = \Delta_1$ , where  $\xi_2$  diverges but  $\xi_1$  is still finite. This point corresponds to a transition to a phase where the activity spreads to the right without limits in a finite fraction of random, and the survival probability tends to a positive limit as  $t \rightarrow \infty$ . At this point and above,  $\tilde{\mu}$  will not exceed  $\tilde{\lambda}$  asymptotically, therefore there is only a partial separation of niveous. As aforementioned, we obtain then no correct information on how the activity spreads rightwards by the SDRG method and it is therefore unable to

predict the properties of this phase transition. The fact that the niveau corresponding to  $\lambda$  does not separate suggests that the transition is, at least, not of activated type characterized by logarithmic time-dependence of observables. Nevertheless, the lowest niveau separates well from the other ones even if  $\Delta \geq \Delta_1$  and in the asymptotic transformation of the corresponding rate  $\kappa$  and that of  $\mu$  the 'incorrect' rate  $\lambda$  does not play a role.

Although we cannot infer the properties of the phase transition, the spreading of the front of the activity started from a single active seed can be related to the distribution of the renormalized recovery rates. If the system is renormalized well beyond the scale  $\xi_1$ , the renormalized backward rates are negligibly small and it behaves as a totally asymmetric contact process, where the recovery rates have a broad distribution with an algebraic tail:

$$P_{<}(\mu) \sim \mu^{1/z}, \quad \mu \rightarrow 0. \quad (37)$$

Assume now that the process was started from a single active seed at  $x(t=0) = 0$  and at time  $t$  there are still active sites. If the leftmost active site, the position of which is denoted by  $x(t)$ , recovers, it will be practically not reinfected and  $x$  is shifted to the closest active site on its right. The expected value of the time of recovery is  $1/\mu_i$ , therefore the mean time  $t_{1,n+1}$  needed for  $x$  to shift from site 1 to site  $n+1$  is at most the sum of recovery times:

$$t_{1,n+1} < \sum_{i=1}^n \mu_i^{-1}. \quad (38)$$

For large  $n$ , the asymptotical behavior of this sum is governed by the exponent  $z$ . If  $z < 1$ ,  $\sum_{i=1}^n \mu_i^{-1} \sim n$ , whereas if  $z > 1$ ,  $\sum_{i=1}^n \mu_i^{-1} \sim n^z$ . This yields the following lower bound on the asymptotical displacement of the leftmost active site:

$$\begin{aligned} x(t) &> O(t) & \text{if } z < 1 \\ x(t) &> O(t^{1/z}) & \text{if } z > 1. \end{aligned} \quad (39)$$

Obviously, the position of the rightmost active site (the front of the activity) must move at least as fast as  $x(t)$  in samples which are surviving up to time  $t$ . If  $\Delta > \Delta_1$ , the forward infection rates are typically larger than the recovery rates in the renormalized model, therefore the density of active sites between  $x(t)$  and the front is expected to be finite, similar to the super-critical phase of the symmetric model. Consequently, if the leftmost active site recovers, the expected shift of  $x(t)$  is finite and the relation in (39) holds as a proportionality.

So, the active cluster moves at least as a power of time, which is different from the behavior of the unbiased model. If  $z > 1$ , which is realized by a weak initial bias, the above reasoning suggests the creeping motion of the critical active cluster with an asymptotically vanishing velocity. This is in contrast to the homogeneous, biased model where the active cluster moves with a finite velocity.

### C. The upper phase transition and the strong-survival phase

If the control parameter  $\Delta$  is further increased in the weak-survival phase ( $\Delta > \Delta_1$ ), the length scale  $\xi_1$ , as well as the dynamical exponent  $z$  increase and, at a second phase transition point  $\Delta = \Delta_2$ , they diverge. Physically, this means that for  $\Delta > \Delta_2$ , the activity, when started from a single active seed spreads also leftwards without limits. In the transition point, the variables  $\omega \simeq \kappa$  and  $\mu$  are dual to each other and the fixed point of the SDRG transformation is an infinite randomness fixed-point with the asymptotic scaling of parameters:

$$|\ln \tilde{\kappa}| \sim |\ln \tilde{\mu}| \sim \xi^{1/2}. \quad (\Delta = \Delta_2) \quad (40)$$

Whereas, above  $\Delta_2$ , we obtain a line of fixed points parameterized by a distribution-dependent dynamical exponent  $z'$ , where the parameters scale as

$$\tilde{\kappa} \sim \xi^{-z'}, \quad |\ln \tilde{\mu}| \sim \xi. \quad (\Delta > \Delta_2) \quad (41)$$

The phase transition at  $\Delta = \Delta_2$  can be also detected in the change of the finite-size scaling of the lowest non-trivial eigenvalue of  $Q$  in a finite, open system of size  $L$ , which is (asymptotically) correctly treated by the SDRG method. The inverse of this quantity that gives the time scale of reaching the absorbing state from the fully active one scales in the following way:

$$\begin{aligned} \tau &\sim L^{\max(1,z)}, & \Delta_1 < \Delta < \Delta_2 \\ \ln \tau &\sim L^{1/2}, & \Delta = \Delta_2 \\ \ln \tau &\sim L, & \Delta > \Delta_2 \end{aligned} \quad (42)$$

Note that in a finite but periodic system, the finite-size scaling of the lowest gap of  $Q$  is different from this. In that case, the extinction time behaves as  $\ln \tau \sim L$  in the entire range  $\Delta > \Delta_1$ , since the activity can 'go around' rightwards and it is irrelevant whether the spreading of infection leftwards is blocked or not. This is consistent with the SDRG treatment. When the periodic system is renormalized up to two effective sites then in the last decimation step the niveau which was the lowest (non-trivial) one till that point and which could indicate the phase transition at  $\Delta_2$  is lost.

As we mentioned above, in the biased model, the renormalized forward rates will be much greater than the backward ones. So, it is plausible to assume that the behavior of the system in the range  $\Delta > \Delta_1$  is well described by a simply tractable idealized model where the forward rates are infinitely large  $\lambda_i = \infty$ . If this process is started from a single active site, the activity will immediately spread to the right without limits, and all sites on the right hand side of the leftmost active site will be active since once a site recovers, its left hand side neighbor will instantly re infect it. It is easy to see that the position  $x(t)$  of the leftmost active site is a random walk with jump rate  $p_i = \mu_i$  and  $q_i = \kappa_{i-1}$  to the right and to the left, respectively if  $x(t) = i$ . The basic properties of

the one-dimensional random walk in a random environment are exactly known, for a review see e.g. Ref. [22]. Varying the control parameter of the problem,

$$\Delta_{\text{RW}} = \overline{\ln q_i} - \overline{\ln p_i}, \quad (43)$$

the expected displacement  $x(t)$  in typical environments has different asymptotics:

$$\begin{aligned} x(t) &\sim t^{1/z} & \Delta_{\text{RW}} < 0 \\ |x(t)| &\sim (\ln t)^2 & \Delta_{\text{RW}} = 0 \\ -x(t) &\sim t^{1/z} & \Delta_{\text{RW}} > 0, \end{aligned} \quad (44)$$

where  $z$  is the positive root of the equation  $\overline{(q_i/p_i)^{1/z}} = 1$  for  $\Delta_{\text{RW}} < 0$ .

So, in the range  $\Delta_1 < \Delta < \Delta_2$ , the position of the leftmost active site is expected to creep rightwards, at  $\Delta = \Delta_2$  to perform a Sinai walk [23] with a zero average displacement and fluctuations in the order of  $(\ln t)^2$ , finally, if  $\Delta > \Delta_2$ , to creep leftwards. These results are consistent with the finite-size scaling of the extinction time given in Eq. (42) and are in line with the behavior of the homogeneous, biased contact process, where  $x(t)$  is a random walk in a homogeneous environment and the extinction time scales at the second transition point as  $\tau \sim L^2$  [24].

The phase transition at  $\Delta = \Delta_2$  can also be detected in the behavior of the survival probability in a semi-infinite system, when the process is started from a single active site (site 0) and infection spreading from this site is not possible to the right, i.e.  $\lambda_0 = 0$ . This quantity can be calculated in the idealized model, where the site on the right hand side of the origin of the random walk will be an absorbing site. The probability  $P(x)$  averaged over the random environments (i.e. sets of transition rates) that the walker visits a site in a distance  $x$  from the origin before it hits the absorbing site is known to be  $O(e^{-\text{const} \cdot x})$ ,  $O(x^{-1/2})$  and constant for  $\Delta_{\text{RW}} < 0$ ,  $\Delta_{\text{RW}} = 0$  and  $\Delta_{\text{RW}} > 0$ , respectively, see e.g. Ref. [25]. Using these results, the asymptotical time-dependence of the survival probability can be derived. If  $\Delta < \Delta_2$ , the activity is localized in the vicinity of the origin but, due to the algebraic tail of the distribution of effective recovery rates in Eq. (37), the survival probability averaged over disorder decays algebraically, as well:

$$P_{\text{surv}}(t) \sim t^{-1/z}. \quad (\Delta < \Delta_2) \quad (45)$$

At the second critical point,  $\Delta = \Delta_2$ , using the relation between time and length scale of the Sinai walk  $\ln t \sim \xi^{1/2}$ , which can be gathered also from the fixed-point solution of the SDRG transformation in Eq. (40), we obtain for the survival probability:

$$P_{\text{surv}}(t) \sim (\ln t)^{-1}. \quad (\Delta = \Delta_2) \quad (46)$$

This form is identical to the surface critical behavior of  $P_{\text{surv}}(t)$  in the unbiased model [13]. An important difference is, however, that the set of active sites is compact

in the biased model, i.e. has a finite density, while in the symmetric model it is a fractal of dimension  $d_f$ .

Finally, for  $\Delta > \Delta_2$ , the survival probability tends to a positive limit that depends on the initial distribution of rates when  $t \rightarrow \infty$ .

## VI. SUMMARY AND OUTLOOK

We have applied an SDRG method to the asymmetric contact process where the infection rates to the left and to the right, as well as the recovery rates are independent random variables. We have shown that the local random asymmetry in the infection spreading is irrelevant on large scales if the model is globally (statistically) symmetric, and the critical and off-critical behavior is identical to that of the disordered, locally symmetric contact process. If the model is globally biased, the SDRG transformation predicts two distinct phase transitions. The lower one is related to the transmission of infection in the direction of the bias. Unlike this transition point, which is out of the range of validity of the method, the upper critical point, which is related to the spreading of activity against the direction of the bias, is controlled by an infinite randomness fixed point.

It would be desirable to check the predictions of the SDRG method by Monte Carlo simulations. An intriguing question which is left open by the SDRG analysis is nature of the lower phase transition. This is predicted to be neither of activated type with logarithmic critical scaling nor to be in the directed percolation class at least for weak asymmetry when the critical cluster is creeping. The present work is restricted to  $d = 1$ , although the critical behavior of the symmetric contact process in the presence of disorder is known to be governed by an infinite randomness fixed-point also in dimensions  $d > 1$  [26–28]. The question of stability of the fixed-point against asymmetry in higher dimensions remains a challenging open problem.

## Acknowledgments

This paper was supported by the János Bolyai Research Scholarship of the Hungarian Academy of Sciences and by the National Research Fund under grant no. K75324.



## Appendix A: The spectrum of the rate matrix

### 1. Two-site block

The rate matrix of a two-site block shown in Fig. 1 is given as:

$$Q_{12} = \begin{pmatrix} 0 & 0 & 0 & 0 \\ \mu_1 & -\mu_1 - \lambda_1 & 0 & \lambda_1 \\ \mu_2 & 0 & -\mu_2 - \kappa_1 & \kappa_1 \\ 0 & \mu_2 & \mu_1 & -\mu_1 - \mu_2 \end{pmatrix}. \quad (\text{A1})$$

The three non-trivial eigenvalues are roots of the cubic equation:

$$\epsilon^3 + a\epsilon^2 + b\epsilon + c = 0, \quad (\text{A2})$$

where

$$\begin{aligned} a &= \lambda_1 + \kappa_1 + 2(\mu_1 + \mu_2) \\ b &= \lambda_1 \kappa_1 + \mu_1 \mu_2 + (\mu_1 + \mu_2)(\mu_1 + \mu_2 + \lambda_1 + \kappa_1) \\ c &= \mu_1 \mu_2 (\mu_1 + \mu_2 + \lambda_1 + \kappa_1). \end{aligned} \quad (\text{A3})$$

### 2. Three-site block

The rate matrix of the three-site block shown in Fig. 2 has a block diagonal form:

$$Q_{123} = \begin{pmatrix} 0 & 0 & 0 & 0 & 0 & 0 & 0 & 0 \\ \mu_2 & -\kappa_1 - \lambda_1 - \mu_2 & 0 & \kappa_1 & 0 & \lambda_2 & 0 & 0 \\ 0 & 0 & -\lambda_1 & \lambda_1 & 0 & 0 & 0 & 0 \\ 0 & 0 & \mu_1 & -\lambda_2 - \mu_1 & 0 & 0 & 0 & \lambda_2 \\ 0 & 0 & 0 & 0 & -\kappa_2 & \kappa_2 & 0 & 0 \\ 0 & 0 & 0 & 0 & \mu_2 & -\kappa_1 - \mu_1 & 0 & \kappa_1 \\ 0 & 0 & 0 & 0 & 0 & 0 & -\lambda_1 - \kappa_2 & \lambda_1 + \kappa_2 \\ 0 & 0 & 0 & 0 & 0 & 0 & \mu_2 & -\mu_2 \end{pmatrix} \quad (\text{A4})$$

and has the following eigenvalues:

$$\epsilon_1 = \epsilon_2 = 0, \quad (\text{A5})$$

$$|\epsilon_{3,4}| = \frac{1}{2}(\mu_2 + \lambda_1 + \lambda_2) \times \left(1 \mp \sqrt{1 - 4\lambda_1\lambda_2/(\mu_2 + \lambda_1 + \lambda_2)^2}\right) \quad (\text{A6})$$

$$|\epsilon_{5,6}| = \frac{1}{2}(\mu_2 + \kappa_1 + \kappa_2) \times \left(1 \mp \sqrt{1 - 4\kappa_1\kappa_2/(\mu_2 + \kappa_1 + \kappa_2)^2}\right) \quad (\text{A7})$$

$$|\epsilon_7| = \mu_2 + \lambda_1 + \kappa_2, \quad |\epsilon_8| = \mu_2 + \lambda_2 + \kappa_1. \quad (\text{A8})$$

- 
- [1] T.E. Harris, Ann. Prob., **2**, 969 (1974).
  - [2] T.M. Liggett, *Stochastic interacting systems: contact, voter, and exclusion processes* (Berlin, Springer, 1999).
  - [3] J. Marro and R. Dickman, *Non-equilibrium phase transitions in lattice models*, Cambridge Univ. Press, (Cambridge 2005).
  - [4] G. Ódor, *Universality in Nonequilibrium Lattice Systems*, World Scientific, 2008; Rev. Mod. Phys. **76**, 663 (2004).
  - [5] M. Henkel, H. Hinrichsen, and S. Lübeck, *Non-equilibrium Phase transitions* (Springer, Berlin 2008).
  - [6] H. Hinrichsen, Physics **2**, 96 (2009).
  - [7] A.J. Noest, Phys. Rev. Lett. **57**, 91 (1986); Phys. Rev. **B 38**, 2715 (1988).
  - [8] A.G. Moreira, R. Dickman, Phys. Rev. E **54**, R3090 (1996).
  - [9] R. Cafiero, A. Gabrielli and M.A. Muñoz, Phys. Rev. E. **57**, 5060 (1998).
  - [10] M. Bramson, R. Durrett, and R.H. Schonmann, Ann. Prob. **19**, 960 (1991).
  - [11] R.B. Griffiths, Phys. Rev. Lett. **23**, 17 (1969); B.M. McCoy, Phys. Rev. Lett. **23**, 383 (1969).
  - [12] F. Iglói and C. Monthus, Phys. Rep. **412**, 277 (2005).

- [13] J. Hooyberghs, F. Iglói, and C. Vanderzande, Phys. Rev. Lett. **90**, 100601 (2003); Phys. Rev. E **69**, 066140 (2004).
- [14] D.S. Fisher Phys. Rev. Lett. **69**, 534 (1992); Phys. Rev. B **51**, 6411 (1995).
- [15] T. Vojta and M. Dickison, Phys. Rev. E **72**, 036126 (2005).
- [16] R.H. Schonmann, J. Stat. Phys. **44**, 505 (1986); T. Sweet, J. Stat. Phys. **86**, 749 (1997).
- [17] A. Costa, R.A. Blythe, and M.R. Evans, J. Stat. Mech. P09008 (2010).
- [18] D.S. Fisher, Phys. Rev. B **50**, 3799 (1994).
- [19] F. Iglói, Phys. Rev. B **65**, 064416 (2002).
- [20] C.J. Neugebauer, S.V. Fallert, and S.N. Taraskin, Phys. Rev. E **74**, 040101(R) (2006); S.V. Fallert and S.N. Taraskin, Phys. Rev. E **79**, 042105 (2009).
- [21] J.A. Hoyos, Phys. Rev. E **78**, 032101 (2008).
- [22] J.P. Bouchaud and A. Georges, Phys. Rep. **195**, 217 (1990).
- [23] Ya.G. Sinai, Theory Probab. Appl. **27**, 256 (1982).
- [24] R. Schinazi, J. Stat. Phys. **74**, 1005 (1994).
- [25] F. Iglói and H. Rieger, Phys. Rev. E **58**, 4238 (1998).
- [26] I.A. Kovács and F. Iglói, Phys. Rev. B **82**, 054437 (2010); Phys. Rev. B **83**, 174207 (2011).
- [27] C. Monthus and T. Garel, J. Stat. Mech. P01008 (2012); arXiv:1206.6997.
- [28] T. Vojta, A. Farquhar, J. Mast, Phys. Rev. E **79**, 011111 (2009); T. Vojta, arXiv:1209.1400.
- [29] This situation is somewhat reminiscent of the difficulties with the renormalization of the random XY chain where both couplings  $J^x$  and  $J^y$  should be larger than the other couplings [18].
- [30] To have a weaker form of complete separation it is sufficient to fulfill the conditions  $\min\{\lambda_1, \lambda_2\} \ll \mu_2$  and  $\min\{\kappa_1, \kappa_2\} \ll \mu_2$ . Then the lowest-lying (non-trivial) eigenvalues are  $O(\min\{\lambda_1, \lambda_2\})$  and  $O(\min\{\kappa_1, \kappa_2\})$ , while the other eigenvalues are  $O(\mu_2)$ .